

MECHANICAL AND MICROSTRUCTURAL/CHEMICAL DEGRADATION
OF COATING AND SUBSTRATE IN GAS TURBINE BLADE

Y. Sugita*, M. Ito*, S. Sakurai#, C. R. Gold+, T. E. Bloomer+ and J. Kameda+

The mechanical property degradation (295-1223 K) and microstructural/chemical evolution of CoNiCrAlY coatings and superalloy substrates in gas turbine blades operated in-service have been studied using a small punch (SP) testing technique and scanning Auger microprobe. In SP tests, coating cracks continuously and discretely propagated at 295 K and higher temperatures, respectively. The ductile-brittle transition temperature of the coatings was increased during long time exposure of gas turbine blades to oxidizing environments while that of the substrate did not change. The low cycle fatigue life of the coatings at 295 K was also reduced in-service. Oxidation and sulfur segregation near the coating surface were found to be major causes of the mechanical degradation of the coatings.

RECEIVED
MAR 08 1996
OSTI

INTRODUCTION

The application of combined cycle steam/gas turbines for electric generation has been increased to improve the fuel efficiency and the environment. It is recognized (1) that mechanical and microstructural/chemical degradation of gas turbine blades made of intermetallic coatings and Ni base superalloy substrates inevitably occurs under high thermal/applied stresses and high temperature oxidation environments. Thus the characterization of the coating and substrate in gas turbine blades is of importance to evaluate the remaining life. However, it is difficult to apply standard testing techniques to investigate the mechanical property degradation of coatings which is highly localized near the surface. A miniaturized small punch (SP) testing method, previously developed for studying temper and radiation embrittlement (2), has been recently proven to have ability to examine the local mechanical properties in amorphous/ceramic coatings on Al alloy substrates (3).

* Electric Power R & D Center, Chubu Electric Power Co., Inc.

Mechanical Engineering Research Laboratory, Hitachi Ltd.

+ Center for Advanced Technology Development, Iowa State University.

MASTER

DISTRIBUTION OF THIS DOCUMENT IS UNLIMITED

This paper attempts to study in-service degradation of the mechanical properties in gas turbine blades using the SP testing technique. Changes in the microstructure and composition of coatings induced during the operation are examined by means of scanning Auger microprobe (SAM). The relationship between the mechanical properties and microstructure/chemistry of the coatings is discussed to evaluate the degree of blade degradation.

EXPERIMENTAL

The present study used gas turbine blades made of a Rene 80 superalloy substrate (Ni: 60.1wt.%, Co: 9.2wt.%, Cr: 13.9wt.%, Al: 3wt.%, Ti: 4.9wt.%, C: 0.15wt.%, B: 0.01wt.%, Mo: 4wt.% and W: 4wt.%) and coating (Ni: 32wt.%, Co: 38.5wt.%, Cr: 21wt.%, Al: 8wt.%, Y: 0.5wt.%). The gas turbine blade had been operated for 8946 h and 21338 h, designated as 9Kh and 21Kh, using combined fuels of kerosene and liquefied natural gas. The coating thickness was varied from 150 to 250 μm .

SP specimens (6 mm ϕ and 0.5 mm thick) and notched SAM specimens (2 mm x 3 mm x 10 mm) were machined from the near surface region of the turbine blades. The coating was located on a side of the SP and SAM specimens. Substrate SP specimens were also prepared by machining off the coating. It was found (4) that SP tests on unpolished coating specimens indicate large data scattering of the compliance and ductility because of the surface roughness and curvature. In order to extract the mechanical properties solely affected by microstructural and chemical factors, therefore, the surface of SP specimens was mechanically polished using emery paper (1000 grid) and alumina powders (0.3 μm).

A puncher with a hemispherical tip (diameter of 2.4 mm) and specially designed specimen holders consisting of lower and upper dies were used for SP tests (2-4). The details of SP loading setup together with a method of measuring the deflection, using a linear voltage capacitance transducer, are shown elsewhere (4,5). SP specimens were placed into the lower die in order that the coating surface could be subjected to tensile applied stresses. The SP specimen, puncher and holder were heated by an induction heating coil. The test temperature was controlled using a thermocouple attached to the lower die. SP tests were performed in air in a temperature range from 295-1223 K using a screw-driven Instron testing machine. The cross head speeds of 2×10^{-5} and 8×10^{-6} m/s were used at 295 K and high temperatures, respectively. The ductility (ϵ_f) was estimated from the critical deflection to cracking (δ_c) obtained from the load vs. deflection curve, using empirical relations (6,7).

The low cycle fatigue (LCF) behavior of the coatings was examined at 295 K using the constant displacement condition ($R = P_{\min}/P_{\max} < 0.05$) and the frequency of 0.1 Hz. The number of cycles to coating cracking (N_f) was determined from plotting the load range ($\Delta P = P_{\max} - P_{\min}$) against the number of fatigue cycles.

SAM analyses were carried out in the unused and used gas turbine blades. Hydrogenated SAM specimens containing notches were fractured in an ultra high vacuum chamber (1.5×10^{-8} Pa) of SAM. Oxides, segregants and alloy compositions on the fracture surfaces were investigated by a cylindrical mirror analyzer (5 keV) of Physical Electronics Model 660. The first derivative Auger peak height of elements was acquired using a survey or window mode. The SAM maps were taken, which correspond to scanning electron microscopy (SEM) micrographs.

RESULTS AND DISCUSSION

Figure 1 shows typical load vs. deflection curves obtained from SP tests on the 9Kh coating specimens at 295 K, 1098 K and 1223 K. A reduction in the loading rate or level off of the load was observed at the critical deflection in the coating and substrate SP specimens. SEM observation on load-interrupted SP specimens at different load levels confirmed that the critical deflection is indicative of crack initiation (4,5). In some coating specimens tested at 1173 K and 1223 K, the formation of ductile cracks was found to cause no changes in the load vs. deflection curve (Fig. 1). In addition, it is shown (4,5) that the yield strength of the coatings decreased with increasing operating time and all the coatings greatly softened at 1223 K.

The temperature dependence of ϵ_f observed in the coating and substrate specimens is indicated in Fig. 2. The data with asterisks mean the strain value at the load-interrupting stage where ductile cracks extended a size of 100-200 μm . Increasing the operating time led to a reduction in the ductility of the coating and substrate at 295 K. All the coatings and unused substrate had lower ductility at 1098 K, compared with those at 295 K. The ductility of the coating and substrate increased with further increasing testing temperature and the ductile-brittle transition behavior was observed. The ductile-brittle transition temperature (DBTT) of the coatings was shifted to higher temperature by 90 K, as a result of the long time operation. The DBTT of the substrate did not change in-service, which remained slightly lower than that of the unused coating. It should be noted that the SP test of the unused substrate demonstrated lower ductility than the tensile test. This finding would be ascribed to the biaxial stress state in the SP test which promotes cracking.

The morphology of coating cracking in SP specimens deformed just above δ_f is shown in Fig. 3. At 295 K, brittle cracks initiated at the center of coating SP specimens and propagated a distance of about 500-1000 μm along the radial direction (Fig. 3a). In SP tests at 1098 K on all the SP specimens, a number of coating cracks were heterogeneously nucleated and discretely grew along either the radial or tangential direction (Fig. 3b). The extension of brittle cracks (50-250 μm) at 1098 K became considerably smaller, compared with that at 295 K. The used coatings revealed longer cracks and a higher crack density than the new coating at 1098 K. Ductile cracks in the unused coating were highly localized near the specimen surface and propagated in a zigzag mode (4,5). In the 9Kh coating strained up to 6 %, as can be seen in Fig. 3c, several coating cracks were initiated at oxides, which had been formed during the operation, and the nucleated cracks extended into the coating matrix accompanied by some crack tip opening.

The LCF behavior of the unused and used coatings was studied using the SP testing technique. Figure 4 indicates the relationship of ΔP to the number of fatigue cycles at the strain range $\Delta\varepsilon = 0.47$ % for the 9Kh coating. The value of ΔP showed +3 % variations. Hardening behavior was observed during LCF in many cases. The formation of coating cracks along the radial direction resulted in a sharp drop in ΔP at the critical number of cycles (N_f) (Fig. 4). Some SP tests showed a gradual load decrease during LCF because of discrete formation of cracks. In such cases, the upper and lower bounds of ΔP provided different values of N_f and the range of N_f was determined (see bars in Fig. 5). The logarithmic plot between N_f and $\Delta\varepsilon$ suggests an empirical relationship, i.e., $N_f = C (\Delta\varepsilon)^{-4.1}$, although some data scattering can be observed (Fig. 5). The power obtained in the present SP tests is a little higher than that in hollow cylinder tests at high temperatures (8). The LCF life tends to decrease, i.e., lowering the value of C , as a result of the long time operation.

In order to clarify the degradation mechanism, fracture surfaces of the coatings were analyzed using SAM. In Figure 6, a SEM micrograph, and oxygen and sulfur maps of the 9Kh coating are revealed. As can be seen in Fig. 6b, oxidation with the form of Al_2O_3 substantially occurred near the coating surface (4,5). Oxides consisting of several alloying constituents were also found near the interface due to the insufficient cleaning during coating processing and they spread into the coating interior during the blade operation (4,5).

Sulfur segregation was clearly observed on fracture surfaces near the surface region of the used coatings (Fig. 6c). The sulfur segregation in the coatings is believed to have occurred in-service because of its absence in the unused coating. The amount of segregated sulfur in some areas reached almost full

monolayer coverage, which has the characteristics of surface segregation rather than those of grain boundary segregation (4,5). Three reasons for the localized sulfur segregation near the coating surface are considered: (i) The alloy composition in a coating region of 100 μm from the interface is highly changed during the operation (4). (ii) Weakly bonded powder/powder interfaces, which serve as strong segregation sites, might remain near the coating surface due to the lack of powder densification. (iii) Sulfur enters into the coating from exterior environments because sulfur was not segregated in coatings thermally aged in air (4).

We now turn to discuss the relationship between the fracture and microstructural/chemical propensities. All the coatings and unused substrate exhibited lower ductility at 1098 K, compared with that at 295 K. Under Ar atmosphere, on the other hand, brittle cracks initiated at higher strains than in air (4). Thus the high temperature degradation of the coatings is considered to be attributed to environmental effects. Hirth and Rice (9) have suggested that diffusive solute, like oxygen at high temperatures, would have stronger interfacial embrittling potency than nondiffusive one. It is possible in intermetallic coatings that absorbed oxygen atoms preferentially diffuse along stressed grain boundaries or interfaces and produce dynamic embrittlement effects at elevated temperatures (10). However, increasing further testing temperature leads to stronger interaction of oxygen with dislocations than with interfaces, as a result of an increase in the dislocation density and tensile stress relaxation. Hence, the dynamic embrittling effect diminishes and the ductile-brittle transition behavior appears. In the used blades, coupling the oxidation and segregated sulfur near the coating surface further promotes brittle cracking and thereby causes the DBTT of the used coatings to increase.

Although the present SP test demonstrated in-service degradation of the ductility and LCF life in the used coatings, the LCF results were more drastically scattered depending on the samples than the DBTT (Figs. 2 and 6). This is probably because the cyclic deformation behavior near the coating surface controlling the LCF life would be strongly affected by the presence of oxides.

CONCLUSION

In-service degradation of the mechanical and metallurgical properties in CoNiCrAlY coatings and Rene 80 substrates of gas turbine blades operated for 8946 h (9Kh) and 21338 h (21Kh) has been examined using a small punch (SP) testing method and scanning Auger analysis. In SP tests, brittle coating cracks continuously and discretely propagated at 295 K and higher temperatures,

respectively. The used coatings indicated a higher ductile-brittle transition temperature by 90 K, compared with the new coating. The low cycle fatigue life of the coatings was reduced as a result of the long time operation as well. High temperature oxidizing attacks resulted in the formation of Al_2O_3 near the surface. Sulfur segregation was remarkably observed on fracture surfaces near the surface region of the used coatings. The fracture property degradation of the coatings induced during the blade operation was found to be attributable to the oxidation and segregated sulfur near the surface.

ACKNOWLEDGMENTS

The authors wish to thank A. H. Swanson for his experimental work at ISU.

REFERENCES

- (1) "Life Assessment and Repair Technology for Combustion Turbine Hot Section Components", Edited by Viswanathan, R. and Allen, J. M., ASM International, Materials Park, OH., 1990.
- (2) Baik, J. M., et al., Scri. Metall., Vol. 17, 1983, pp. 1143.
- (3) Kameda, J. and Ranjan, R., Mater. Sci. Eng., Vol. A183, 1994, pp. 124.
- (4) Kameda, J., et al., "Degradation Characterization of Coatings and Substrates in Gas Turbine Blades", Contract Report, Center for Advanced Technology Development, Iowa State University, 1995.
- (5) Sugita, Y., et al., "ASME Turbo Expo '95", in press and "Coatings and Substrate Integrity of High Temperature Materials", Edited by Cheruvu, N. S., Swaminathan, V. P. and Liaw, P. K., TMS, Warrendale, PA, submitted.
- (6) Mão, X. and Takahashi, H., J. Nucl. Mater., Vol. 150, 1987, pp. 42.
- (7) Kameda, J. and Mao, X., J. Mater. Sci., Vol. 27, 1992, pp. 983.
- (8) Bernstein, H. L., et al., "Thermomechanical Fatigue Behavior of Materials", ASTM STP 1186, Edited by Sehitoglu, H., American Society for Testing Materials, Philadelphia, PA, 1993, pp. 212.
- (9) Hirth, J. P. and Rice, J. R., Metall. Trans. A, Vol. 11A, 1980, pp. 1501.
- (10) Liu, C. T. and White, C. L., Acta Metall., Vol. 35, 1987, pp. 643.

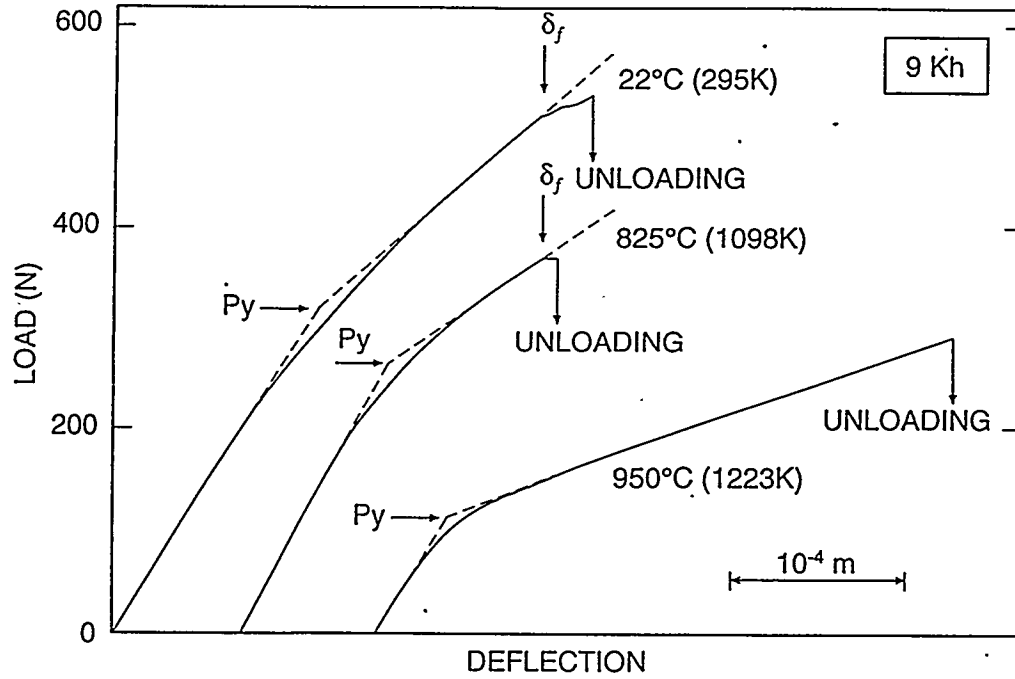


Figure 1. Typical load vs. deflection curves obtained from SP tests on 9Kh SP coating specimens at 295 K, 1098 K and 1223 K.

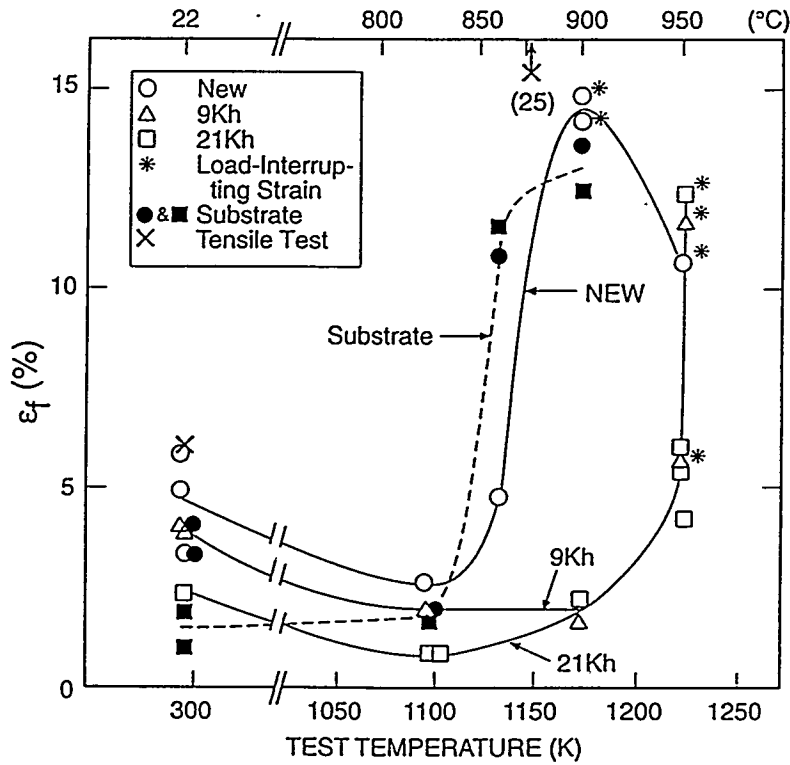


Figure 2. Temperature dependence of fracture strain (ϵ_f) obtained from SP tests on new and used coatings and substrates, compared with tensile test results.

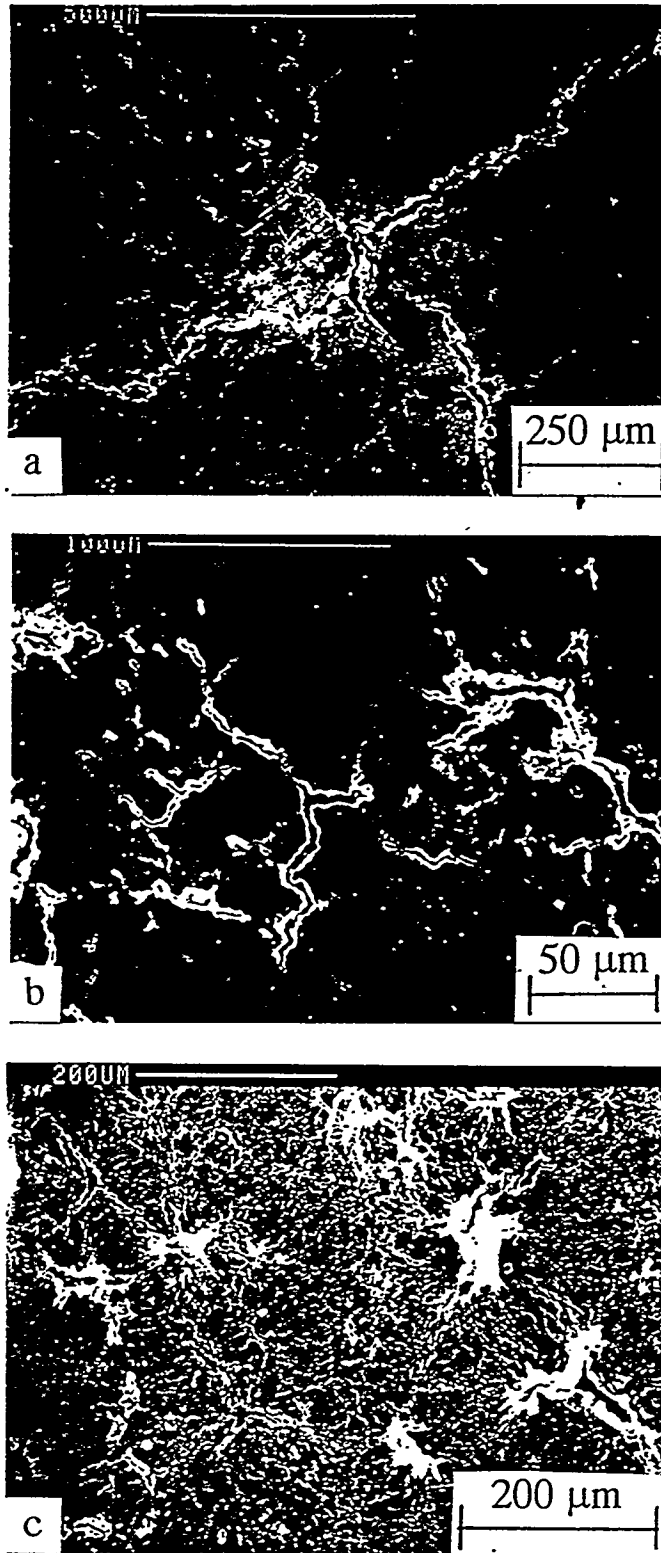


Figure 3. SEM micrographs of cracking morphology (a) at 295 K in unused coating, (b) at 1098 K in 21Kh coating and (c) 1223 K in 9Kh coating.

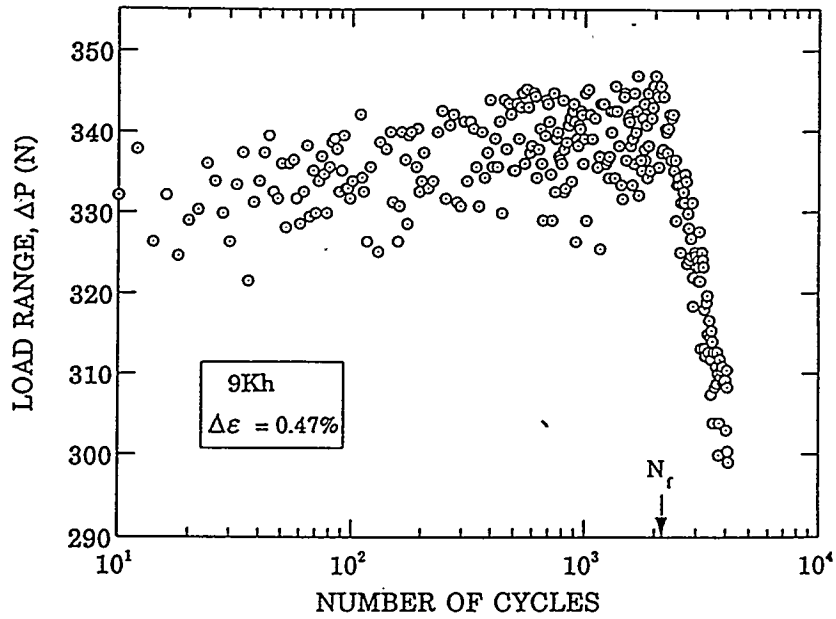


Figure 4. Variation of load range with number of fatigue cycles at $\Delta \epsilon = 0.47\%$ in 9Kh coating.

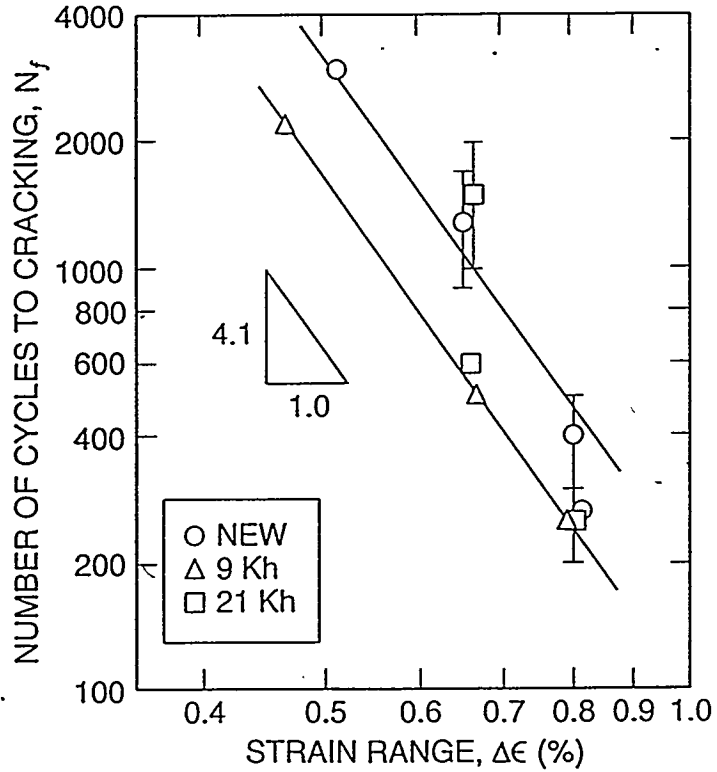


Figure 5. Logarithmic relationship between number of fatigue cycles to coating cracking (N_f) and strain range ($\Delta \epsilon$).

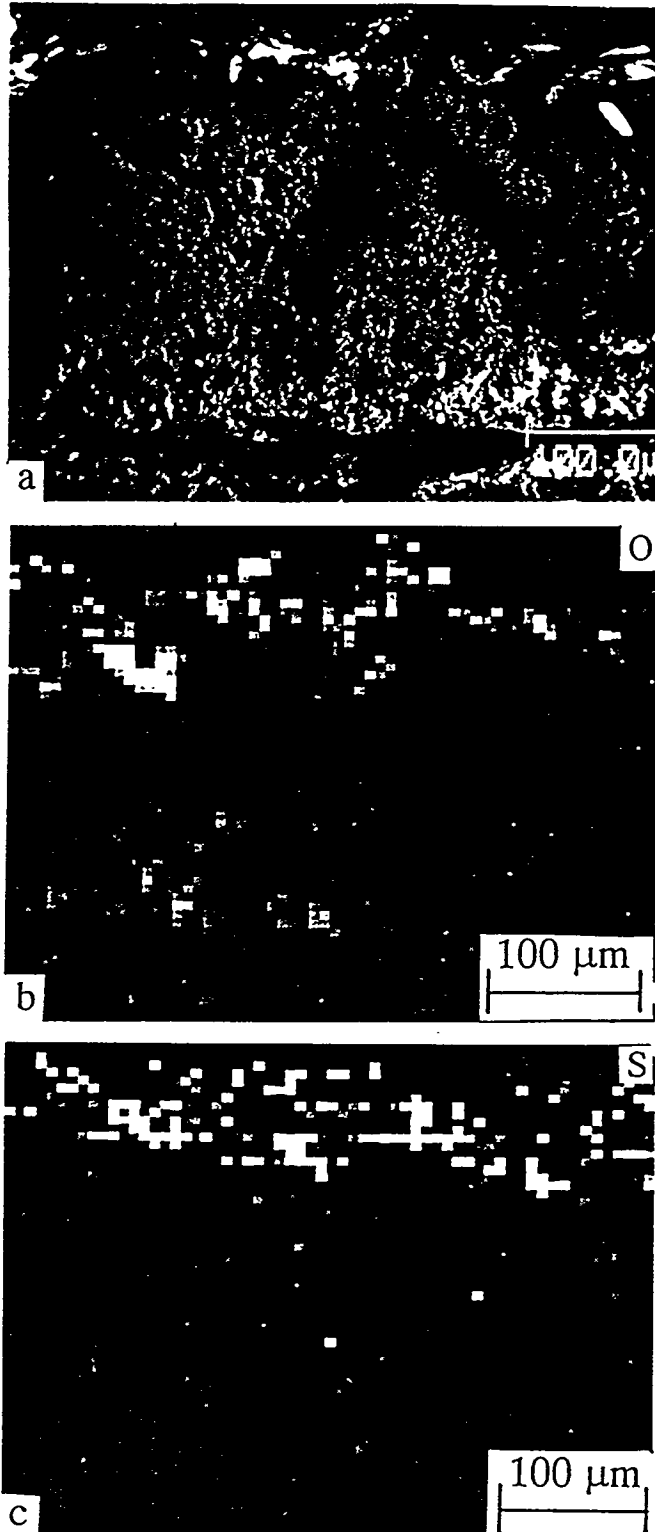


Figure 6. (a) SEM micrograph, and (b) oxygen and (c) sulfur maps on fracture surfaces of 9Kh coating and substrate near interface.

DISCLAIMER

This report was prepared as an account of work sponsored by an agency of the United States Government. Neither the United States Government nor any agency thereof, nor any of their employees, makes any warranty, express or implied, or assumes any legal liability or responsibility for the accuracy, completeness, or usefulness of any information, apparatus, product, or process disclosed, or represents that its use would not infringe privately owned rights. Reference herein to any specific commercial product, process, or service by trade name, trademark, manufacturer, or otherwise does not necessarily constitute or imply its endorsement, recommendation, or favoring by the United States Government or any agency thereof. The views and opinions of authors expressed herein do not necessarily state or reflect those of the United States Government or any agency thereof.